



Experimental Hysteresis Identification and Micro-position Control of a Shape-Memory-Alloy Rod Actuator

S. A. Mir Mohammad Sadeghi, S. F. Hoseini, A. Fathi*, H. Mohammadi Daniali

Department of Mechanical Engineering, Babol Noshirvani University of Technology, Babol, Iran

PAPER INFO

Paper history:

Received 03 August 2018

Received in revised form 04 November 2018

Accepted 03 January 2019

Keywords:

Shape-Memory-Alloy Actuator

Wiener Model

System Identification

Position Control

PID tuning

Particle Swarm Optimization

ABSTRACT

In order to exhaustively exploit the high-level capabilities of shape memory alloys (SMAs), they must be applied in control systems applications. However, because of their hysteretic inherent, dilatory response, and nonlinear behavior, scientists are thwarted in their attempt to design controllers for actuators of such kind. The current study aims at developing a micro-position control system for a novel SMA rod actuator. To do so, the hysteretic behavior of the actuator was simulated in the form of a gray-box Wiener model. Based on the experimental training dataset obtained from the actuator, the hysteresis Wiener model was trained using a PSO algorithm. Afterwards that the identified hysteresis Wiener model was validated, the authors formed a model-in-the-loop (MIL) position control system. Next, a PSO algorithm was again set to find the best controller parameters regarding some performance criteria. At the end, implemented on the fabricated prototype (the experimental setup), the designed control system shared such excellent accuracy that makes the fabricated actuator amenable to micro-positioning applications.

doi: 10.5829/ije.2019.32.01a.09

1. INTRODUCTION

Shape memory alloy (SMA) actuators are capable of reshaping to their memorized shape when heated, which makes them suit a broad variety of applications such as robotics, medicine, surgical tools, and so on. However, because of the multiple non-smooth nonlinearities associated with the hysteretic inherent of them, scientists have difficulties modeling and controlling them. On the other hand, un-modeled hysteresis may lead to an imprecision in trajectory tracking and, hence, a deterioration in performance of the control system. To overcome this limitation, it is necessary to develop a hysteresis model that shares the essential features of SMA actuators and be suitable enough for model-in-the-loop (MIL) control systems as well as real-time implementations. Roohbakhsh Davaran and Sadrnejad [1] proposed a constitutive, integrated model for SMAs capable of predicting three-dimensional behaviors. A great deal of research has been geared towards identifying the hysteresis behavior of SMAs using intelligent methods [2-5]. Towards further

commercializing SMA actuators, Jani et al. [6] have conducted a review research. Once one overcomes the inherent complexities of SMAs, then can enjoy such a diverse applicability of SMAs. Noroozi and Sadrnezhaad [7] have utilized NiTiNol wires to fabricate a spring stent prototype used for opening the femoral vessels. Sayyadi and Zakerzadeh [8] have nonlinearly modelled a flexible beam actuated by two SMA wires. Designing control systems for SMAs can provide scientists with substantial benefits. Elahinia et al. [9, 10] have investigated shape-memory-alloy actuated control systems by reviewing many controller-design problems. Barforoushi et al. [11] have developed a linear SMA actuator by reducing its hysteresis nonlinearity using the inverse of the modified Prandtl-Ishlinskii (PI) model. Intelligent optimization algorithms have been of huge aid in designing PID controllers [12-15]. Ahn and Kha [16] have used a Genetic Algorithm (GA) to tune controllers for SMA actuators by using and the Preisach hysteresis model [16]. In this study, a user-friendly paradigm is presented towards developing a micro-position control system for a fabricated SMA rod actuator. To do so, PSO algorithm

*Corresponding Author Email: fathi@nit.ac.ir (A. Fathi)

was used for identifying the hysteresis grey-box wiener model and for designing a PID controller for the actuator prototype. In comparison with similar existing actuators, this actuator is jubilant of having huge force to stroke ratio. Additionally, it can provide high forces up to 20N in such a limited spaces, which makes it a great candidate for a wide spectrum of applications. What follows next in the article shall be organized as follows: the next section will introduce the structure of the fabricated actuator along with the experimental setup. Next, section 3 is dedicated to the modeling of the hysteresis behavior of the actuator. Section 4 demonstrates how to identify the obtained hysteresis model by using experimental data. Section 5 discusses the results obtained. At last, the conclusion of the article is given in section 6.

2. FABRICATED ACTUATOR AND EXPERIMENTAL SETUP

Similar previous works analyze SMA wires as embedded actuators, yet the actuator used in this study includes a NiTiNol bended double-support rod. According to Figure 1, a compression spring is set to make the backward motion possible. The actuation process can be described as follows: Firstly, a compression spring causes a deformation in the actuator (the bended form). When the electrical currents pass through the connecting wires, the SMA rod is heated up and phase transformation begins, and it forms its memorized, straight shape. When electrical current is cut off, the rod is cooled down, due to the heat convection with the ambient, and the compression spring bends it back, ready to begin the next cycle. The actuator provides a motion with a 5-mm stroke, and it produces forces up to 20N. It is of real importance that the spring is to be designed optimally so that it provides a reciprocating motion the forward and return strokes of which are at the same pace. To prepare the identification data, an experimental setup was provided including the SMA actuator, a data acquisition card, a Linear Variable Differential Transformer (LVDT) sensor, a programmable power supply, and a personal computer (PC). The LVDT sends the linear displacement to the PC via the data acquisition card. Figure 2 shows the experimental setup.

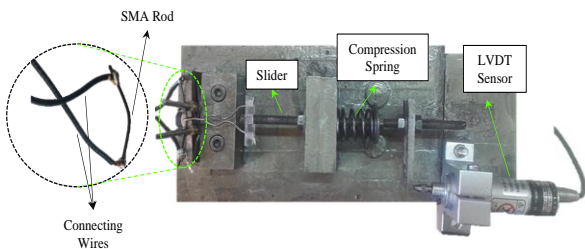


Figure 1. The fabricated SMA rod actuator

The data acquisition card is a USB 8 Channel 49 kHz 12-bit A/D from EAGLE technology. The power supply is a programmable switching DC from Good Will Instrument Co., and it is connected to the PC via an RS232 cable. The LVDT sensor is of DLH-A-5mm model from DACell Company. The fabricated actuator is a candidate for the applications such as Robotics, Medicine, and so on [17-19].

3. SMA MODELLING

The concept of the Wiener model has been taken advantage for modeling the hysteresis behavior [20]. Thereafter, by using a PSO algorithm and an experimental training dataset, the authors trained and validated the hysteresis Wiener model. Generally, a Wiener model comprises a series connection of a linear dynamic block and a nonlinear static block. A very useful trait of models of such kind is the ease of controller design as well as high potential for real-time implementation. As can be seen from Figure 3, the linear dynamic block characterizes the system dynamic behavior such as the response speed and the time delay, and, the nonlinear static block defines hysteresis phase transformation and mechanical deformation of the alloy. In this study, the heat transfer model of cyclic thermal response plays role as the linear dynamic block. The hysteresis block predicts the martensite volume fraction (ξ) of the alloy at a specific temperature (T).

The simplified one-dimensional heat transfer equation describing the SMA actuator for resistive heating and ambient air-cooling is expressed as follows [21-23]:

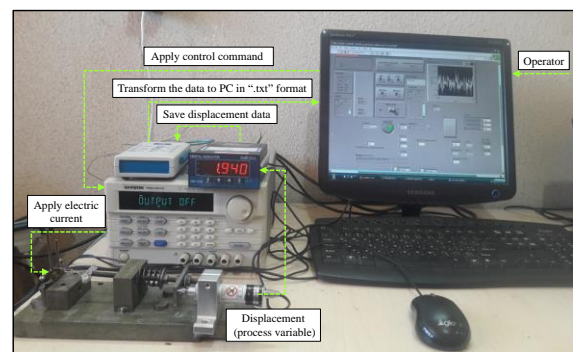


Figure 2. The setup prepared for the experimental tests

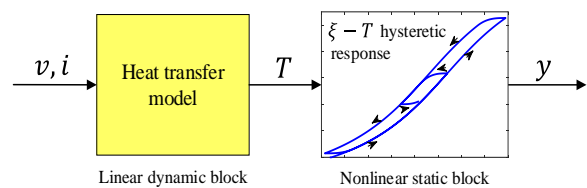


Figure 3. The configuration of the Wiener model

$$mC_p \left(\frac{dT}{dt} \right) = \begin{cases} i^2 R - hA(T - T_a); & \text{heating} \\ -hA(T - T_a); & \text{cooling} \end{cases} \quad (1)$$

where, $m = \rho\pi^2 d/4$ is the SMA rod mass per unit length, ρ denotes density, d denotes the rod diameter, C_p denotes specific heat capacity, T and T_a denote the rod and the ambient temperature, respectively. i is the applied current, R is the rod resistance per unit length, h is convective heat transfer coefficient for the ambient cooling conditions, $A = \pi dl$ designates the convective surface area of the rod, and l is the rod length. The above heat transfer expression is based on some assumptions that follows: the heat transfer effect is one dimensional; the applied load to the actuator is gradual/constant; radiation effects is negligibly small in comparison with the conduction mode; T_a , R , and h remain constant; the rod temperature field is of spatial uniform type; and phase transformation temperatures are assumed constants. In the range of temperature below 200 °C, which applies here, the effect of heat radiation is negligible [24]. By solving Equation (1), the rod maximum temperature T can be obtained for the heating and cooling process

$$T - T_a = \begin{cases} (T_i - T_a)e^{-t/\tau} + i^2 \lambda (1 - e^{-t/\tau}); & \text{heating} \\ (T_i - T_a)e^{-t/\tau}; & \text{cooling} \end{cases} \quad (2)$$

where T_i denotes the rod temperature at the time t ; besides, $\tau \equiv mC_p/hA$ and $\lambda \equiv R/hA$ are referred to as time constant and current constant, respectively. Finally, using Equation (2), the electrical current required for heating the actuator to the temperature T is found to be

$$i_{\text{heating}} = \sqrt{\frac{(T - T_a) - (T_i - T_a)e^{-t/\tau}}{\lambda(1 - e^{-t/\tau})}} \quad (3)$$

When the actuator is heated, the phase transformation, and hence the shape change, begins, which makes the temperature pass A_s (austenite start temperature) and end at A_f (austenite finish temperature). In addition, in order for the actuator to be fixed at the actuated position, the temperature must be maintained above A_f by the application of optimal power [25]. Eventually, the represented heat transfer model plays the role of the linear block in modeling the behavior of the SMA actuator.

3. 2. The $\xi - T$ Hysteretic Response of SMAs

Hysteresis trajectories are mostly inside the limiting major loop formed by the combination of the descending and ascending curves. De Almeida et al. [26] and Nascimento et al. [27] proposed the following function for the $\xi(T)$ behavior (see Figure 4).

$$\xi(T, \delta) = F_L(T) \Delta \frac{2\xi_s}{\pi} \left[\arctan\left(\frac{T - \delta T_c}{h_0}\right) \right] + \xi_0 \quad (4)$$

where T is the excitation temperature, ξ_0 is the saturation martensite, ξ_s is the hysteresis height, T_c is the critical temperature at the center of the hysteresis curve, and h_0 is a constant depending on the material. In addition, $\delta = \text{sgn}(\dot{T})$. The major hysteresis loop in the ξ - T plane is described by the combination of the curves of $F_L(T, \delta = +1)$ and $F_L(T, \delta = -1)$. However, in order to describe reversal curves, minor loops, and nested minor loops in and to represent the dependence $\xi(T)$ for any trajectory inside the limiting major loop, a modification must be done on Equation (4). To do so, it is of real importance to consider the way in which the inner trajectories approach the limiting major loop. T_p is the proximity temperature and is defined to estimate the distance between the current point (T_L, ξ) on the curve $F_L(T, \delta)$ and is given as follows:

$$T_p \Delta T_L - T \quad (5)$$

Using Equation (4) to find T_L corresponding to $\xi = F_L(T_L, \delta = +1)$ leads to:

$$T_L = h_0 \tan\left(\frac{\pi\xi}{2\xi_s}\right) + \delta T_c \quad (6)$$

Therefore, T_p at (T_0, ξ_0) is found as:

$$T_p = h_0 \tan\left(\frac{\pi\xi_0}{2\xi_s}\right) + \delta T_c - T \quad (7)$$

At the beginning of a new trajectory emanating from the reversal point (T_r, ξ_r) , the proximity function T_p is called as T_{pr} and obtained as follows:

$$T_{pr} = h_0 \tan\left(\frac{\pi\xi_0}{2\xi_s}\right) + \delta T_c - T_r \quad (8)$$

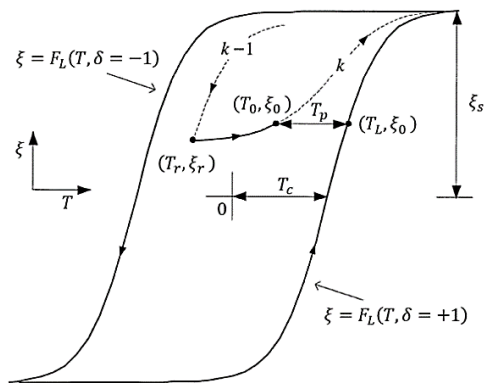


Figure 4. Schematic representation of hysteresis in $\xi - T$ characteristics [26]

Consequently, in order to describe T_p for any branch in the major loop, a functional dependence is presented as follows:

$$T_p \Delta T_{Pr} P(x) \tag{9}$$

where

$$x \Delta \left(\frac{T - T_r}{T_{Pr}} \right) \tag{10}$$

Therefore, the martensite at any point (T, ξ) and for a hysteresis branch which is reversed at the point (T_r, ξ_r) inside the major T - ξ loop is formulated as follows:

$$\xi(T) = \frac{2\xi_s}{\pi} \left[\arctan \left(\frac{T_{Pr} P\left(\frac{T - T_r}{T_{Pr}}\right) + T - \delta T_c}{h_0} \right) \right] \tag{11}$$

The following proximity function is given for an employed SMA rod [26]:

$$P(x) \Delta \begin{cases} 1 - \sin \zeta x; & \zeta x < \frac{\pi}{2} \\ 0; & \zeta x > \frac{\pi}{2} \end{cases} \tag{12}$$

4. SYSTEM IDENTIFICATION

Wiener model can be used to model a variety of systems, especially those whose static and dynamic responses can be analyzed independently. In this study, in order to identify the unknown parameters of the nonlinear hysteresis block, a PSO algorithm was used [28, 29]. The unknown constants to be identified are $R, hA, T_r, h_0,$ and T_c , where the former two are related to Equation (1), and the latter three are related to Equation (8). The experiment-based hysteresis identification process of the SMA actuator is illustrated in Figure 5. Firstly, a training input is fed to both the SMA actuator and to the hysteresis Wiener model. Next, the mean squared error (MSE) between the target and the system output is minimized by the PSO algorithm [2]. The schematic diagram of the experiment-based hysteresis identification of the actuator is shown in Figure 5.

The setting parameters of PSO algorithm are chosen as follows: maximum number of iterations=150, number of particles=50. $w, c_1,$ and c_2 are set, respectively, equal to 0.9, 2, and 2. The decision variables $R, hA, T_r, h_0,$ and T_c are, respectively, limited to the lower bound of [0, 0, -10, 0.1, 0.1] and to the upper bound of [2, 3, 0, 2, 2]. The obtained hysteresis model is shown in Figure 6. Figure 7 illustrates the training of the hysteresis model compared to the experimental measurement. Now that the hysteresis model is trained, it must be validated. Figure 8

depicts the validation procedure of the developed hysteresis model.

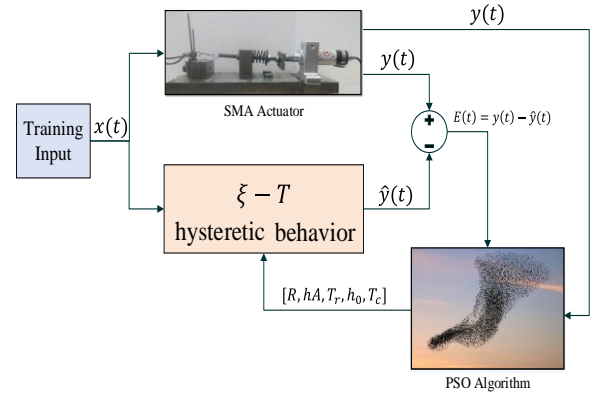


Figure 5. Experimental hysteresis system identification of the SMA actuator

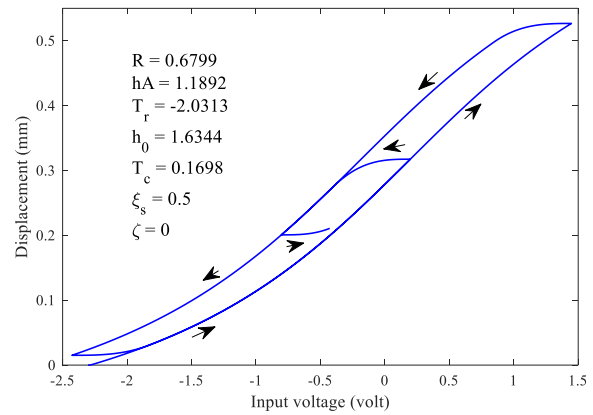


Figure 6. The identified hysteresis model

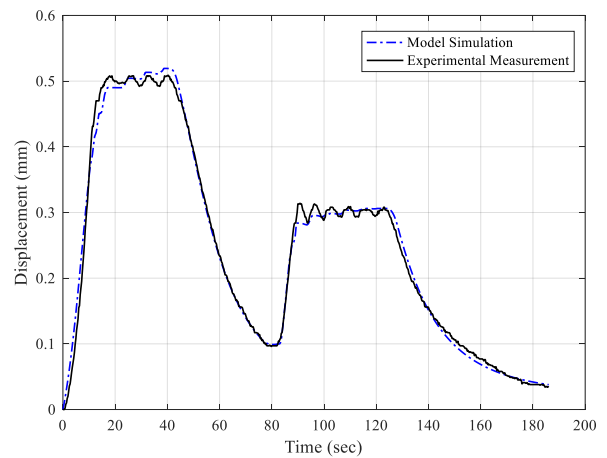


Figure 7. Training of the hysteresis model using the experimental data

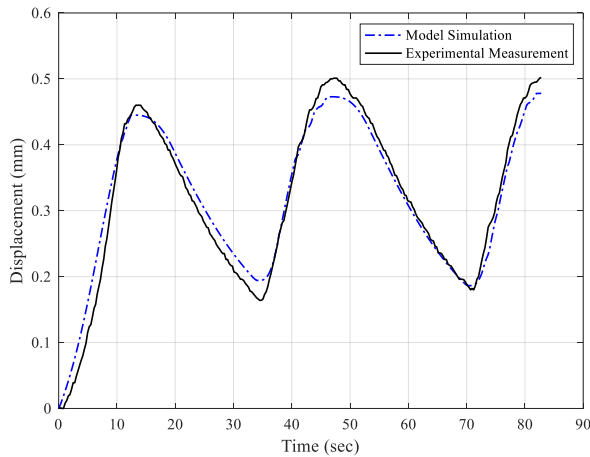


Figure 8. Validation of the hysteresis model using the experimental data

5. RESULTS AND DISCUSSION

In order to achieve an accurate micro-position control system, the parameters of the PID controller must be optimally tuned. Knowing that the identified hysteresis model is successfully capable of approximating the experimental data, the authors have designed an MIL position control system, and they had a PSO algorithm tune the PID controller, as shown in Figure 9. The current saturation block might evoke concern whether the proposed model is in danger of trapping in limit cycles. By using the describing-function method as well as frequency response analysis, it has been ascertained that there exist no limit cycles jeopardizing the model stability. The objective function that is to be minimized is given as follows:

$$f = \vec{w} * \{MSE, Energy, RiseTime, T_s, \%OS\} \tag{13}$$

where

$$Energy = \frac{1}{2} \int_1^n u_i^2 dt \tag{14}$$

where n is the total size of the simulation; u_i is the i -th sample of the control effort signal. \vec{w} is a five-by-one scaling vector, which balances the dimensions of the objectives. The PSO algorithm setting parameters are set as follows: maximum number of iterations=150, number of particles=50; in addition, w , c_1 , and c_2 are decided based on constriction coefficients. The decision variables (Kp , Ki , and Kd) are limited to the upper bound of [500, 1, 1] and to the lower bound of [0, 0, 0], respectively. Eventually, after meeting the termination criterion, the PSO algorithm offered the solution to be $Kp = 202.5604$, $Ki = 0.0169$, and $Kd = 0$. Therefore, the values of $Kp = 200$, $Ki = 0.01$, and $Kd = 0$ were finalized to be the solution to the problem discussed in this article. This controller was implemented in the SMA actuator. It should be noted that in the experimental tests the sampling time is 0.287 s. Figure 10 illustrates the response of the controlled actuator to a step reference of 0.5 mm. The response of the actuator to a sinusoidal electric current is shown in Figure 11. In order to balance the speed at which the actuator settles to a positive and a negative peak, a similar returning SMA actuator may be used. The developed micro-position SMA rod actuator can be used in the applications such as medicine, robotics, and so on. The experiment-based hysteresis identification and the PSO-PID control strategy are straightforward and suit best to industrial applications. Besides, this user-friendly strategy can be readily applied to any SMA actuators. What mentioned previously may be left as challenging topics for further expansion of the current study in the future.

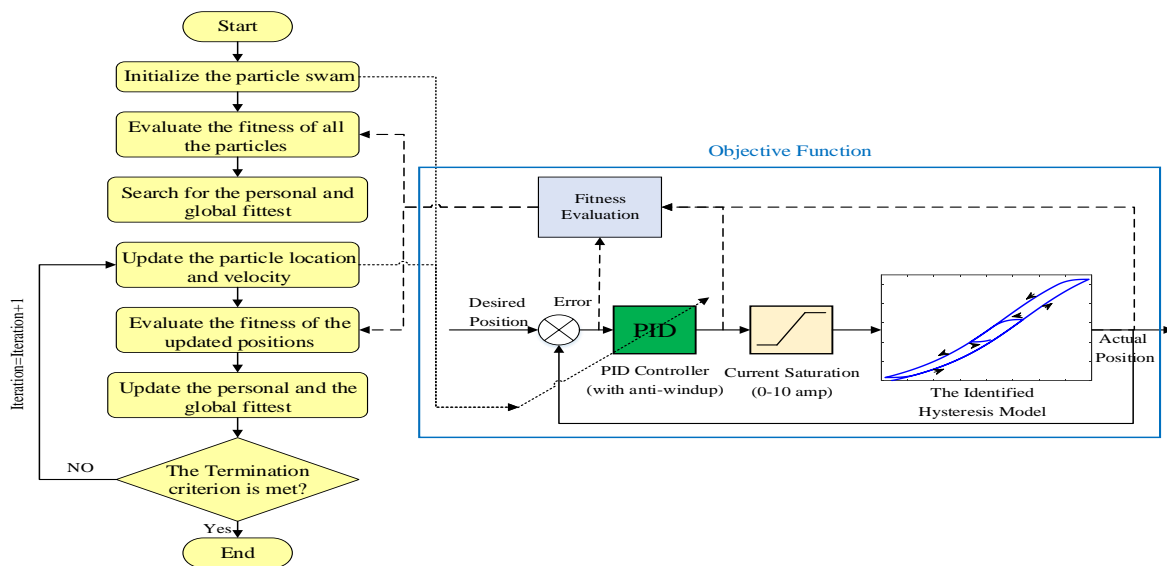


Figure 9. Flowchart of PSO algorithm linked to the MIL position control system

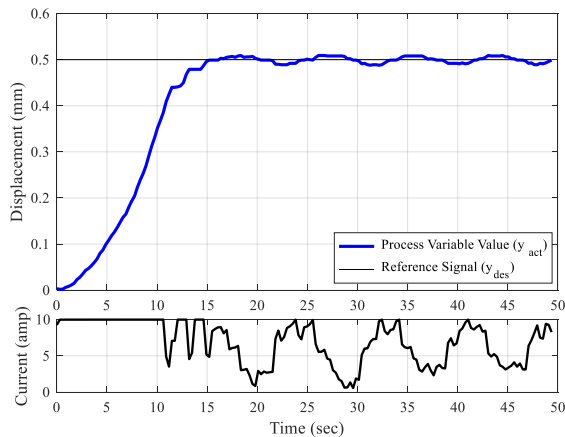


Figure 10. Position control of the actuator to the set point of 0.5 mm

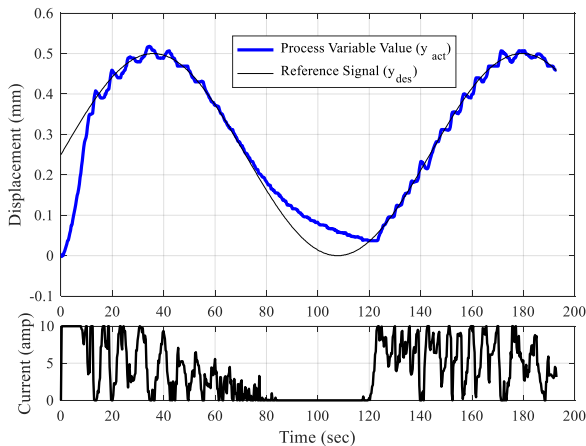


Figure 11. Position control of the actuator prototype to a 0.007-Hz sinusoidal input

6. CONCLUSIONS

It is of real significance to design control systems for SMA actuators due to their complicated behavior. In this study, the hysteresis behavior of an SMA rod actuator was modeled using an experiment-based identification of Wiener model. Next, this identified model has been used to form an MIL position control system of the actuator. Afterwards, a PSO algorithm was recruited to find the best PID controller gains by minimizing the desired performance indices of the closed loop MIL system. According to the experimental results, it can be concluded that the developed position control system is a strong candidate for micro-position control applications.

7. REFERENCES

1. Roohbakhsh Davaran, A. and Sadrnejad, S.A., "A 3d micro-plane model for shape memory alloys", *International Journal of Engineering-Transactions A: Basics*, Vol. 21, No. 1, (2007), 17-30.
2. Fathi, A. and Mozaffari, A., "Identification of a dynamic model for shape memory alloy actuator using hammerstein-wiener gray box and mutable smart bee algorithm", *International Journal of Intelligent Computing and Cybernetics*, Vol. 6, No. 4, (2013), 328-357.
3. Mozaffari, A., Fathi, A. and Azad, N.L., "Preferred design of recurrent neural network architecture using a multiobjective evolutionary algorithm with un-supervised information recruitment: A paradigm for modeling shape memory alloy actuators", *Meccanica*, Vol. 49, No. 6, (2014), 1297-1326.
4. Jokar, M., Ayati, M., Yousefi-Koma, A. and Basaeri, H., "Experiment-based hysteresis identification of a shape memory alloy-embedded morphing mechanism via stretched particle swarm optimization algorithm", *Journal of Intelligent Material Systems and Structures*, Vol. 28, No. 19, (2017), 2781-2792.
5. Shakiba, S., Zakerzadeh, M.R. and Ayati, M., "Experimental characterization and control of a magnetic shape memory alloy actuator using the modified generalized rate-dependent prandtl-ishlinskii hysteresis model", *Proceedings of the Institution of Mechanical Engineers, Part I: Journal of Systems and Control Engineering*, Vol. 232, No. 5, (2018), 506-518.
6. Mohd Jani, J., Leary, M. and Subic, A., "Designing shape memory alloy linear actuators: A review", *Journal of Intelligent Material Systems and Structures*, Vol. 28, No. 13, (2017), 1699-1718.
7. Noroozi, S. and Sadrnezhad, S., "Fabrication of spiral stent with superelastic/shape memory nitinol alloy for femoral vessel", *International Journal of Engineering-Transactions A: Basics*, Vol. 30, No. 7, (2017), 1048-1053.
8. Sayyaadi, H. and Zakerzadeh, M.R., "Nonlinear analysis of a flexible beam actuated by a couple of active sma wire actuators", *International Journal of Engineering-Transactions C: Aspects*, Vol. 25, No. 3, (2012), 249-264.
9. Elahinia, M., Esfahani, E. and Wang, S., Control of sma systems: Review of the state of the art, 2010.
10. Elahinia, M.H., "Shape memory alloy actuators: Design, fabrication, and experimental evaluation, John Wiley & Sons, (2016).
11. Barforoushi, S.D., Fathi, A. and Danaee, S., "Experimental model of shape memory alloy actuators using modified prandtl-ishlinskii model", *UPB Buletin Stiintific, Series B: Chemistry and Materials Science*, Vol. 73, No. 2, (2011), 255-266.
12. Sarvi, M., Derakhshan, M. and Sedighzadeh, M., "A new intelligent controller for parallel DC/DC converters", *International Journal of Engineering-Transactions A: Basics*, Vol. 27, No. 1, (2013), 131-142.
13. Mahmoudzadeh, S., Mojallali, H. and Pourjafari, N., "An optimized pid for capsubots using modified chaotic genetic algorithm (Research Note)", *International Journal of Engineering-Transactions C: Aspects*, Vol. 27, No. 9, (2014), 1377-1384.
14. Ara, A.L., Tolabi, H.B. and Hosseini, R., "Dynamic modeling and controller design of distribution static compensator in a microgrid based on combination of fuzzy set and galaxy-based search algorithm", *International Journal of Engineering-Transactions A: Basics*, Vol. 29, No. 10, (2016), 1392-1400.
15. MirMohammadSadeghi, S.A., Nikzadfar, K., Bakhshinezhad, N. and Fathi, A., "Optimal idle speed control of a natural aspirated gasoline engine using bio-inspired meta-heuristic algorithms", *International Journal of Automotive Engineering*, Vol. 8, No. 3, (2018), 2792-2806.
16. Ahn, K.K. and Kha, N.B., "Modeling and control of shape memory alloy actuators using preisach model, genetic algorithm and fuzzy logic", *Mechatronics*, Vol. 18, No. 3, (2008), 141-152.

17. Hadi, A., Alipour, K., Kazeminasab, S. and Elahinia, M., "Asr glove: A wearable glove for hand assistance and rehabilitation using shape memory alloys", *Journal of Intelligent Material Systems and Structures*, Vol. 29, No. 8, (2018), 1575-1585.
18. Nematollahi, M., Mehrabi, R., Callejas, M.R., Elahinia, H. and Elahinia, M., "A two-way architectural actuator using niti se wire and sme spring", in *Active and Passive Smart Structures and Integrated Systems XII*, International Society for Optics and Photonics, Vol. 10595, (2018).
19. Kazeminasab, S., Hadi, A., Alipour, K. and Elahinia, M., "Force and motion control of a tendon-driven hand exoskeleton actuated by shape memory alloys", *Industrial Robot: An International Journal*, Vol. 45, No. 5, (2018), 623-633.
20. Villoslada, A., Flores, A., Copaci, D., Blanco, D. and Moreno, L., "High-displacement flexible shape memory alloy actuator for soft wearable robots", *Robotics and Autonomous Systems*, Vol. 73, (2015), 91-101.
21. Potapov, P.L. and Da Silva, E.P., "Time response of shape memory alloy actuators", *Journal of Intelligent Material Systems and Structures*, Vol. 11, No. 2, (2000), 125-134.
22. Meier, H. and Oelschlaeger, L., "Numerical thermomechanical modelling of shape memory alloy wires", *Materials Science and Engineering*, Vol. A 378, No. 1-2, (2004), 484-489.
23. Bhattacharyya, A., Sweeney, L. and Faulkner, M., "Experimental characterization of free convection during thermal phase transformations in shape memory alloy wires", *Smart materials and Structures*, Vol. 11, No. 3, (2002), 411-422.
24. Kohl, M., "Shape memory microactuators", Springer Science & Business Media., (2013).
25. Sreekumar, M., Nagarajan, T. and Singaperumal, M., "Application of trained niti sma actuators in a spatial compliant mechanism: Experimental investigations", *Materials & Design*, Vol. 30, No. 8, (2009), 3020-3029.
26. De Almeida, L.A.L., Deep, G.S., Lima, A.M.N. and Neff, H., "Limiting loop proximity hysteresis model", *IEEE Transactions on magnetics*, Vol. 39, No. 1, (2003), 523-528.
27. Nascimento, M., De Araújo, C., De Almeida, L., Da Rocha Neto, J. and Lima, A., "A mathematical model for the strain-temperature hysteresis of shape memory alloy actuators", *Materials & Design*, Vol. 30, No. 3, (2009), 551-556.
28. Naitali, A. and Giri, F., "Wiener-hammerstein system identification—an evolutionary approach", *International Journal of Systems Science*, Vol. 47, No. 1, (2016), 45-61.
29. Eberhart, R. and Kennedy, J., "A new optimizer using particle swarm theory", In *Proceedings of the Sixth International Symposium on Micro Machine and Human Science*, IEEE, (1995), 39-43.

Experimental Hysteresis Identification and Micro-position Control of a Shape-memory-alloy Rod Actuator

S. A. Mir Mohammad Sadeghi, S. F. Hoseini, A. Fathi, H. Mohammadi Daniali

Department of Mechanical Engineering, Babol Noshirvani University of Technology, Babol, Iran

P A P E R I N F O

چکیده

Paper history:

Received 03 August 2018

Received in revised form 04 November 2018

Accepted 03 January 2019

Keywords:

Shape-Memory-Alloy Actuator

Wiener Model

System Identification

Position Control

PID tuning

Particle Swarm Optimization

برای بهره‌برداری کامل از توانایی‌های سطح بالا از آلیاژهای حافظه شکل (SMAs)، آن‌ها باید در برنامه‌های کاربردی سیستم‌های کنترل اعمال شوند. با این حال، به علت پاسخ هیسترتیک، پاسخ دایمی و رفتار غیرخطی، دانشمندان در تلاش برای طراحی کنترل‌کننده‌ها برای محرک‌های چنین نوعی از بین می‌روند. مطالعه حاضر با هدف ایجاد یک سیستم کنترل موقعیت میکرو برای یک سیم پیچ جدید SMA توسعه یافت. برای انجام این کار، رفتار هیسترتی‌کننده محرک در قالب مدل وینر خاکستری جعبه شیشه‌سازی شد. بر اساس داده‌های آموزشی تجربی حاصل از محرک، مدل هیسترتیز وینر با استفاده از الگوریتم PSO آموزش داده شد. پس از آن که مدل هیسترتیز Wiener شناسایی گشت اعتبار سنجی شده، و نویسندگان یک سیستم کنترل موقعیتی مدل (in-the-loop) (MIL) را ایجاد کردند. بعد، یک الگوریتم PSO دوباره برای یافتن بهترین پارامترهای کنترل در رابطه با برخی از معیارهای عملکرد تنظیم شد. در نهایت، بر اساس نمونه اولیه ساخته شده (نصب آزمایشی)، سیستم کنترل طراحی شده، چنین دقت عالی را به وجود آورد که باعث می‌شود سازنده تولید شده بتواند به برنامه‌های موقعیت‌یابی میکرو تبدیل شود.

doi: 10.5829/ije.2019.32.01a.09